AD-A131 630 THEORETICAL ANALYSIS OF NONRECIPROCAL ELECTROMAGNETIC SURFACE WAVE DEVICES(U) HARRY DIAMOND LABS ADELPHI MD C A MORRISON ET AL. SEP 83 HDL-TR-2017 1/1

UNCLASSIFIED F/G 20/14 NL

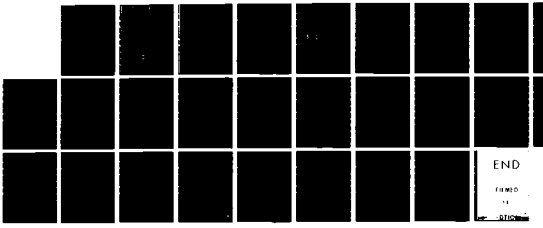

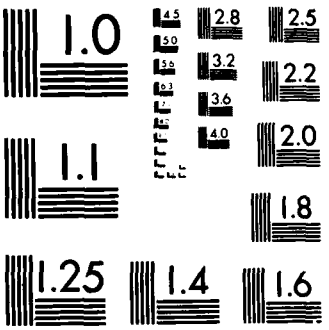

(12)

HDL-TR-2017

September 1983

Theoretical Analysis of Nonreciprocal Electromagnetic Surface Wave Devices

by Clyde A. Morrison
Amanda F. Hansen
Karla M. Sorenson

U.S. Army Electronics Research and Development Command
Harry Diamond Laboratories
Adelphi, MD 20783

Approved for public release; distribution unlimited.

The findings in this report are not to be construed as an official Department of the Army position unless so designated by other authorized documents.

Citation of manufacturers' or trade names does not constitute an official indorsement or approval of the use thereof.

Destroy this report when it is no longer needed. Do not return it to the originator.

UNCLASSIFIED

SECURITY CLASSIFICATION OF THIS PAGE (When Data Entered)

REPORT DOCUMENTATION PAGE	READ INSTRUCTIONS BEFORE COMPLETING FORM
1. REPORT NUMBER HDL-TR-2017	2. GOVT ACCESSION NO. / 3. RECIPIENT'S CATALOG NUMBER
4. TITLE (and Subtitle) *Theoretical Analysis of Nonreciprocal Electromagnetic Surface Wave Devices*	5. TYPE OF REPORT & PERIOD COVERED Technical Report 6. PERFORMING ORG. REPORT NUMBER
7. AUTHOR(s) *Clyde A. Morrison* Amanda F. Hansen Karla M. Sorenson	8. CONTRACT OR GRANT NUMBER(s)
9. PERFORMING ORGANIZATION NAME AND ADDRESS Harry Diamond Laboratories 2800 Powder Mill Road Adelphi, MD 20783	10. PROGRAM ELEMENT, PROJECT, TASK AREA & WORK UNIT NUMBERS Program Element 61101A
11. CONTROLLING OFFICE NAME AND ADDRESS U.S. Army Materiel Development and Readiness Command Alexandria, VA 22333	12. REPORT DATE September 1983 13. NUMBER OF PAGES 37
14. MONITORING AGENCY NAME & ADDRESS (if different from Controlling Office)	15. SECURITY CLASS. (of this report) UNCLASSIFIED 15a. DECLASSIFICATION/DOWNGRADING SCHEDULE

16. DISTRIBUTION STATEMENT (of this Report)

Approved for public release; distribution unlimited.

17. DISTRIBUTION STATEMENT (of the abstract entered in Block 20, if different from Report)

18. SUPPLEMENTARY NOTES

DRCMS Code: 61110191A0011
DA No. 1L161101A91A
HDL Project No. A103C4

19. KEY WORDS (Continue on reverse side if necessary and identify by block number)

Ferrite
Isolators
Phase shifter

20. ABSTRACT (Continue on reverse side if necessary and identify by block number)

An investigation of the possibility of building a low applied magnetic field isolator or nonreciprocal phase shifter at 90 GHz or at higher frequencies is given. The structure consists of a ferrite slab backed by a metal plate. A magnetic field is applied in the plane of the ferrite slab. By solving Maxwell's equations, including the equation of motion of magnetization, we show that under appropriate conditions surface waves on the structure can exist. We further show that for different ferrite slab thicknesses and different applied magnetic fields, only waves travelling along the slab transverse to the applied magnetic field can exist. With the results isolators can be

DD FORM 1 JAN 73 1473 EDITION OF 1 NOV 65 IS OBSOLETE

UNCLASSIFIED

SECURITY CLASSIFICATION OF THIS PAGE (When Data Entered)

20 Abstract (Cont.)

constructed. Since thicker slabs allow surface waves to propagate in both directions with different phase velocities, we have the elements of a phase shifter

CONTENTS

APPENDICES

FIGURES

FIGURES (Cont'd)

1. INTRODUCTION

The recent interest in the near-millimeter-wave region of the electromagnetic spectrum has created a need for attenuators, phase shifters, isolators, and other devices at these frequencies. Attempts to scale standard ferrite devices from the X band (9 GHz) to this frequency range are frustrated by the requirement of high static magnetic fields. At X band the magnetic field required for ferromagnetic resonance is approximately 3,000 gauss (G*)[1] while at 90 GHz the field required for ferromagnetic resonance is approximately 30,000 G. Such high fields are difficult to generate for use in practical, portable devices. One method of overcoming this obstacle is to use ferrites with large internal fields. Then the resonance can be achieved by applying a modest external field.[2] However, such ferrite materials generally have a relatively large intrinsic loss and this leads to devices that have a large and undesirable insertion loss. We wish to develop a new technique of using conventional, low-loss ferrite material in an unconventional manner to produce the necessary devices at near-millimeter wavelengths.

In this report we investigate the possibility of building a low applied magnetic field isolator or nonreciprocal phase shifter at 90 GHz or at higher frequencies using standard, low-loss ferrites. The system studied is shown in figure 1. It consists of a thin ferrite slab backed by a metal plate. The static applied magnetic field is in the plane of the ferrite slab. Solutions to Maxwell's equations, including the equation of motion of magnetization, are given. These equations are applied to the particular geometry, and it is shown that under appropriate conditions only the dominant surface wave mode propagates. The dominant surface wave is the transverse electric (TE) surface mode with the electric vector parallel to the static magnetic field. Conditions on the slab thickness are found such that only the dominant TE mode propagates. As the static magnetic field is increased from zero, the phase of the forward wave (waves propagating along the positive y-axis), differs from the phase of the backward wave (waves propagating along the negative y-axis), and this can be used as a nonreciprocal phase shifter. If the static magnetic field is increased and an appropriate slab thickness is chosen, one of the waves, either the forward or reverse wave, is cut off, and this can be used as an isolator. Furthermore, conditions on the slab thickness and static magnetic field can be found such that neither forward nor reverse waves propagate. The field strength can then be changed, and one of the waves will propagate. Thus, by changing the applied magnetic field suddenly, we have a switching device.

---

[1] *B. Lax and K. J. Button, Microwave Ferrites and Ferrimagnetics, McGraw Hill, New York (1962). [This book contains a large number of practical applications of ferrites to microwave devices. Much of the pioneer work on yttrium iron garnet single crystals and applications of ferrites to microwave devices was done at Harry Diamond Laboratories. Reference to this work is contained in the selected bibliography section.]*

[2] *W. H. Von Aulock, Handbook of Microwave Ferrite Materials, Academic Press, New York (1965), p 451.*

**(gauss) = (tesla) × 10^{-4}*

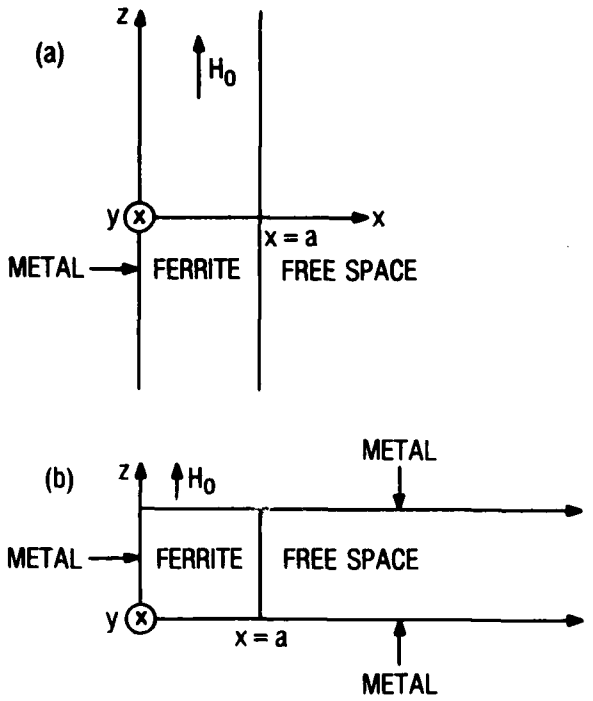

Figure 1. Coordinate system for two geometries applicable to present analysis.

2. *THEORY*

In general, Maxwell's equations (in cgs units) when the fields vary harmonically as $e^{-i\omega t}$ are[3]

$$\nabla\times\mathbf{E} = ik\mathbf{B} \quad ,$$

$$\nabla\times\mathbf{H} = -ik\mathbf{D} + \frac{4\pi}{c}\mathbf{J} \quad ,$$

$$\nabla\cdot\mathbf{B} = 0 \quad , \qquad (1)$$

and

$$\nabla\cdot\mathbf{D} = 4\pi\rho$$

with

$$k = \omega/c \quad .$$

For our purposes, we shall assume that $\mathbf{J}$ and ρ are zero; thus, the electric field, $\mathbf{E}$, and the electric displacement, $\mathbf{D}$, are related by

$$\mathbf{D} = \varepsilon\mathbf{E} \quad . \qquad (2)$$

With these assumptions and equation (2), we have

$$\nabla\cdot\mathbf{E} = 0$$

and (3)

$$\nabla\times\mathbf{H} = -ik\varepsilon\mathbf{E} \quad .$$

The configurations we have chosen are shown in figure 1. The analysis is equally applicable to the configuration of figure 1a or figure 1b. We assume that none of the fields vary in the z direction, and we assume a TE mode in the structure ($E_x = E_y = 0$, $E_z \neq 0$). With these assumptions, the first of equations (1) can be written as

$$\frac{\partial}{\partial y} E_z = ikB_x$$

and (4)

$$-\frac{\partial}{\partial x} E_z = ikB_y \quad .$$

---

[3] *J. D. Jackson, Classical Electrodynamics, second edition, Wiley, New York (1975), p 217.*

In appendix A we obtain the **B**, **H** relationship

$$B_x = \mu H_x + i\kappa H_y \quad ,$$

and (A-13)

$$B_y = \mu H_y - i\kappa H_x \quad ,$$

When these relations are used in equation (4) we get

$$\frac{\partial}{\partial y} E_z = ik\left(\mu H_x + i\kappa H_y\right)$$

and (5)

$$-\frac{\partial}{\partial x} E_z = ik\left(\mu H_y - i\kappa H_x\right) \quad .$$

The results given in equation (5) can be used to determine the magnetic fields as

$$H_x = \left(\mu \frac{\partial}{\partial y} E + i\kappa \frac{\partial}{\partial x} E_z\right)/\left[ik\left(\mu^2 - \kappa^2\right)\right]$$

and (6)

$$H_y = -\left(\mu \frac{\partial}{\partial x} E_z - i\kappa \frac{\partial}{\partial y} E_z\right)/\left[ik\left(\mu^2 - \kappa^2\right)\right] \quad .$$

Equation (6) determines the magnetic field components once the electric field, E_z, is known. To determine E_z, we must obtain the wave equation satisfied by this field component.

To obtain the wave equation for E_z we take the curl of the first of equations (1),

$$\nabla\times\nabla\times\mathbf{E} = ik\nabla\times\mathbf{B}$$

and in Cartesian coordinates

$$\nabla(\nabla.\mathbf{E}) - \nabla^2\mathbf{E} = ik(\nabla\times\mathbf{B}) \quad .$$

From equation (3) and since **E** has only a z component, we obtain

$$-\nabla^2 E_z = ik\left(\frac{\partial}{\partial y} B_x - \frac{\partial}{\partial x} B_y\right) \tag{7}$$

where

$$\nabla^2 = \frac{\partial^2}{\partial x^2} + \frac{\partial^2}{\partial y^2} \quad .$$

The result on the right side of equation (7) can be reduced by using equation (A-13) and $\nabla\cdot\mathbf{B} = 0$ to obtain

$$\nabla^2 E_z + k^2 \frac{\varepsilon}{\mu}\left(\mu^2 - \kappa^2\right)E_z = 0 \quad . \tag{8}$$

This is the wave equation satisfied by E_z for the region occupied by the ferrite slab. To obtain the corresponding wave equation for the exterior region ($x > a$), let $\kappa = 0$ and $\varepsilon = \mu = 1$ in equation (8); thus

$$\nabla^2 E_z + k^2 E_z = 0, \quad x > a \quad . \tag{9}$$

If we assume that we have a wave propagating along the y-axis so that all the fields vary as e^{iqy}, then equations (8), (9), and (6) can be written as

$$\frac{d^2}{dx^2} E + \left[k^2 \frac{\varepsilon}{\mu} \left(\mu^2 - \kappa^2\right) - q^2\right] E = 0 \quad , \qquad 0 < x < a \quad ,$$

$$\frac{d^2}{dx^2} E + \left(k^2 - q^2\right) E_z = 0 \quad , \qquad x > a \quad ,$$

$$H_x = \left(q\mu E + \kappa \frac{dE}{dx}\right) / \left[k\left(\mu^2 - \kappa^2\right)\right] \quad , \qquad 0 < x < a \quad ,$$

$$H_x = \frac{q}{k} E \quad , \qquad x > a \quad , \tag{10}$$

$$H_y = -\left(\mu \frac{dE}{dx} + q\kappa E\right) / \left[ik\left(\mu^2 - \kappa^2\right)\right] \quad , \qquad 0 < x < a \quad ,$$

and

$$H_y = \frac{-1}{ik} \frac{dE}{dx} \qquad x > a \quad ,$$

where

$$E_z = E e^{iqy} \quad .$$

The nonreciprocal term appears in H_y, in the product $q\kappa$. If the magnetic field is reversed, $\kappa\left(-H_o\right) = -\kappa\left(H_o\right)$ (see eq (A-14) and (A-11), app A), then H_y returns to the same form if we reverse the direction of propagation. That is,

$$q\kappa\left(H_o\right) = (-q)\kappa\left(-H_o\right) \quad . \tag{11}$$

However, the results given in equations (11) and (10) are not sufficient to assure nonreciprocity. To achieve a truly nonreciprocal device it is necessary to have some asymmetry in the x direction. For the case considered here, the asymmetry is supplied by the conductor at $x = 0$. Asymmetry could also be supplied by replacing the conductor by a dielectric slab. The solution for a dielectric slab is considerably more complicated than for the conducting plate considered here, but the problem using a dielectric slab may be more useful for a practical device.

We wish to have surface waves propagating along the ferrite slab, so we assume solutions for equation (10) of the form

$$E = A \sin(\Gamma_i x) \quad , \qquad 0 < x < a \quad ,$$

and (12)

$$E = Be^{-\Gamma_o x} \quad , \qquad x > a \quad ,$$

where

$$\Gamma_i^2 = k^2\varepsilon(\mu^2 - \kappa^2)/\mu - q^2$$

and

$$\Gamma_o^2 = q^2 - k^2 \quad .$$

The corresponding magnetic fields are obtained using equation (10). The boundary condition at $x = 0$ is that $E_z = 0$, and the solution chosen, in equation (12), assures that this boundary condition is satisfied. The boundary conditions at the surface of the slab ($x = a$) are that E_z a H_y are continuous. Using equations (12) and (10), and applying these bou. ry conditions, we obtain

$$-\Gamma_o = [q\kappa + \mu\Gamma_i \cot(\Gamma_i a)]/(\mu^2 - \kappa^2) \quad . \tag{13}$$

This is the transcendental equation determining the propagation cons t q, if the relationships of q with Γ_o and Γ_i given in equation (12) are used.

In our discussion of equation (11) we pointed out that the nonreciprocity arises due to the product $q\kappa$. This is also true in equation (13). If we express Γ_o and Γ_i in terms of q, using equation (12), the only unknown in equation (13) is q. All the quantities in equation (13) are even functions of the magnetic field (μ, Γ_i, and Γ_o), except that κ is an odd function of magnetic field ($\kappa(-H_o) = -\kappa(H_o)$). Thus, if we find the solution of equation (13) for H_o positive (q_+) and the solution of H_o negative (q_-) assuming q positive in both cases, then $\Delta q = q_+ - q_-$ would be the differential phase shift. The same result could be obtained by assuming first q positive, then q negative, but the magnetic field $H_o > 0$ in both cases. Because of the complicated manner in which the magnetic field enters in equation (13), we would expect this differential phase shift, Δq, to vary with the strength of the static magnetic field, H_o. Thus, by varying the applied magnetic field, H_o, the differential phase shift can be varied.[1]

3. COMPUTATION

For the purposes of numerical evaluation it is convenient to introduce several dimensionless variables

$$\Gamma_o = k\gamma_o \quad ,$$

$$\Gamma_i = k\gamma_i \quad ,$$

[1] *B. Lax and K. J. Button, Microwave Ferrites and Ferrimagnetics, McGraw Hill, New York (1962). [Detailed descriptions of various nonreciprocal phase shifters are given in the later chapters of this work.]*

(14)

and

$$q = k\sigma \quad .$$

Using these variables introduced by equation (14) in equation (13) we obtain

$$-\gamma_o = \left[\sigma\kappa + \mu\gamma_i \cot\left(ka\gamma_i\right)\right]/\left(\mu^2 - \kappa^2\right) \quad , \tag{15}$$

and equation (12) becomes

$$\gamma_o^2 = 1 - \sigma^2 \quad ,$$

and (16)

$$\gamma_i^2 = \varepsilon\left(\mu^2 - \kappa^2\right)/\mu - \sigma^2 \quad .$$

The solutions of equations (15) and (16) then give the dimensionless quantities γ_o, γ_i, and σ for any particular ferrite. Because of the complicated nature of these equations, it is extremely difficult to obtain a solution, particularly when magnetic losses and dielectric losses are considered. We shall restrict ourselves to the lossless case. Losses in a dielectric slab ($H_o = 0$ in eq (15)) are considered in appendix B.

The lossless case for the magnetic part is given by letting $\alpha = 0$ in equations (A-11) and (A-14). If we assume that the dielectric constant is real (to consider losses in the dielectric, we assume $\varepsilon = \varepsilon' + i\varepsilon''$, with $\varepsilon'' > 0$), then the roots of equation (16) are all real. A useful result can be obtained from equation (15) if we investigate the limit $\gamma_o \to 0^+$ (that is, $\Gamma_o \to 0^+$). This situation corresponds to the limit where the surface wave on the ferrite is minimally bound. If we let $\gamma_o = 0$ in equation (15) we have

$$\kappa + \mu\gamma_i \cot\left(ka\gamma_i\right) = 0 \quad , \tag{17}$$

and for $\gamma_o = 0$ equation (16) yields

$$\begin{aligned} \sigma &= 1 \quad , \\ \gamma_i &= \left[\varepsilon\left(\mu^2 - k^2\right)/\mu - 1\right]^{1/2} \quad , \end{aligned} \tag{18}$$

and since equation (17) is even in γ_i, we need only consider solutions for which $\gamma_i > 0$. The solution of equation (17) for $ka\gamma_i$ is given by

$$ka\gamma_i = \tan^{-1}\left(\frac{-\mu\gamma_i}{\kappa}\right) + p\pi \quad , \tag{19}$$

where $p = 0, 1, 2, \ldots$ (Actually p can take on negative values, but for our purposes $p \geq 0$ is sufficient.) The value of p in equation (19) is the smallest integer that makes the right side positive (larger positive values of

p give higher modes). Since γ_i is given by equation (18), equation (19) gives the thickness, a, of the ferrite slab for a particular value of magnetic field, H_o. Thus we have

$$a_+ = \frac{1}{k\gamma_i}\left[\tan^{-1}\left(-\frac{\mu\gamma_i}{\kappa}\right) + p_+\pi\right] \quad , \tag{20}$$

and if we let $H_o \to -H_o$ we have

$$a_- = \frac{1}{k\gamma_i}\left[\tan^{-1}\left(\frac{\mu\gamma_i}{\kappa}\right) + p_-\pi\right] \quad , \tag{21}$$

since $\kappa(-H_o) = -\kappa(H_o)$.

For the lossless case ($\alpha = 0$) using equations (A-14) and (A-11), we can write the quantities entering equations (21) and (18) as

$$\mu^2 - \kappa^2 = \frac{(H_1 - B)(H_1 + B)}{(H_1 - H_2)(H_1 + H_2)} \quad ,$$

$$\frac{\kappa}{\mu} = -\frac{4\pi M H_1}{(H_1 - H_2)(H_1 + H_2)}$$

and

$$\mu = 1 + \frac{4\pi M H}{H^2 - H_1^2} \quad ,$$

where

$$B = H + 4\pi M \quad ,$$

$$H_2 = \sqrt{BH} \quad ,$$

$$H_1 = \omega/\gamma \quad .$$

The analytical form corresponding to a Brillouin function[4] for spin 1/2 particles

$$M(H) = M_o \tanh(sH) \quad , \tag{22}$$

is assumed with s chosen by assuming M(H) to be 90 percent of the saturation magnetization, M_o, at a field of 500 Oe.*

The slab thickness, a_+, for magnetic fields in the positive z direction given in equation (20) with the smallest value of p_+ gives the lowest mode cutoff. That is, any slab thinner than a_+ will be cut off. The higher modes

[4] *C. Kittel, Introduction to Solid State Physics, fourth edition, Wiley, New York (1971), p 505.*

**(Oe) = (A/m) × 79.577*

are given by larger values of p_+ in equation (20). The slab thickness given in equation (21) is for the magnetic field in the negative z direction. The resulting thicknesses, a_+ and a_-, for the lowest mode for yttrium iron garnet (YIG) are shown in figure 2. The frequency chosen is 90 GHz and the properties of YIG are from Von Aulock.[2] From figure 2 we see that at H_o = 3000 Oe, for a slab thicker than 283 μm, radiation propagates in both directions. With H_o = 3000 Oe and for a slab between 283 and 276 μm, only waves propagating in the positive y direction are allowed and we have an isolator. For slabs less than 276 μm and a field of 3000 Oe, no wave propagates. Therefore, curves as given by figure 2 can be used to design isolators, switches, and nonreciprocal phase shifters for ferrite materials, provided the material has low dielectric and magnetic losses. Even in cases where these losses are not negligible, data as presented in figure 2 are helpful for design purposes, provided operating points are chosen as far as possible from the cutoff points. Figure 3 shows the slab thicknesses a_+ and a_- for a nickel zinc ferrite at 90 GHz. The slab thicknesses are reduced because of the larger dielectric constant ($\varepsilon \simeq 12.5$ as compared to $\varepsilon \simeq 10$ for YIG). The differential thickness given by

$$\Delta a = a_- - a_+ \tag{23}$$

is increased because of the larger saturation magnetization ($4\pi M_o \simeq 1750$ G for YIG, $4\pi M_o \simeq 5000$ G for nickel zinc ferrite). In both figures 2 and 3, the low applied magnetic field values ($H_o < 500$ Oe in fig. 2 and $H_o < 1000$ Oe in fig. 3) should not be given too much consideration.

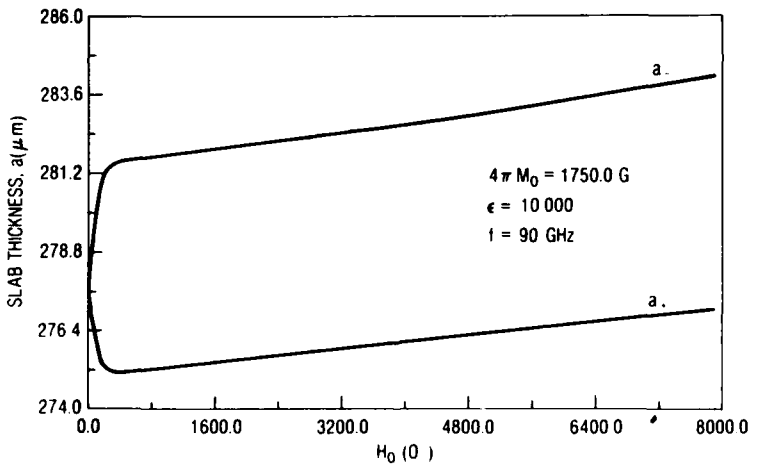

Figure 2. Slab thickness as a function of magnetic field for $Y_3Fe_5O_{12}$ (YIG) with reported values at X-band frequencies.

[2] *W. H. Von Aulock, Handbook of Microwave Ferrite Materials, Academic Press, New York (1965), p 451.*

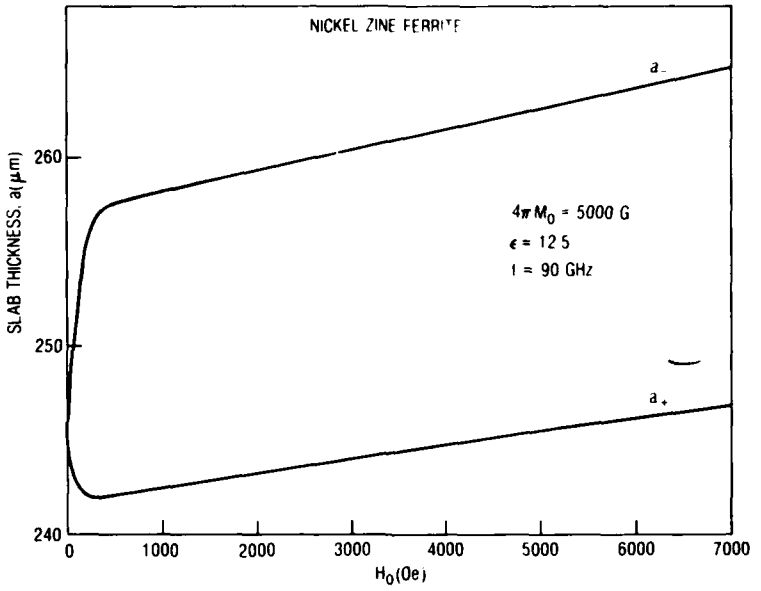

Figure 3. Slab thickness as a function of magnetic field for nickel-zinc ferrite.

To illustrate more clearly the effect of changing only one of the variables of a material, such as the dielectric constant or saturation magnetization, several hypothetical cases are considered using the values for YIG as a starting point. In figure 4 the dielectric constant of the ferrite is increased to 12 from the original value (10) used in figure 2. The results show that thinner slabs are required for similar behavior, but that the differential thickness, Δa, remains essentially unchanged from its original value in figure 2. Increasing the dielectric constant to 14 has essentially the same effect, as can be seen in figure 5. With the dielectric constant at 10 but with the saturation magnetization increased from 1750 (in fig. 2) to 2000 G, the calculations are repeated and the results are shown in figure 6. Comparing these results with those in figure 2, we see that there is only a slight change in the differential thickness, Δa. Since the saturation magnetization changes with temperature,[2] the results shown in figure 6 indicate that an isolator would not be very sensitive to changes in the ambient temperature. Figures 7 and 8 have larger departures of the saturation magnetization from the value of 1750 G used in figure 2. They show that the differential thickness increases with saturation magnetization, but the slab thickness is essentially constant for changes in $4\pi M$. Therefore, the results given in figures 2 through 8 would indicate that, to a good approximation, we can assume that increasing the dielectric constant decreases the required slab thickness and increasing the saturation magnetization increases the differential thickness. These two effects are independent.

---

[2] *W. H. Von Aulock, Handbook of Microwave Ferrite Materials, Academic Press, New York (1965), p 451.*

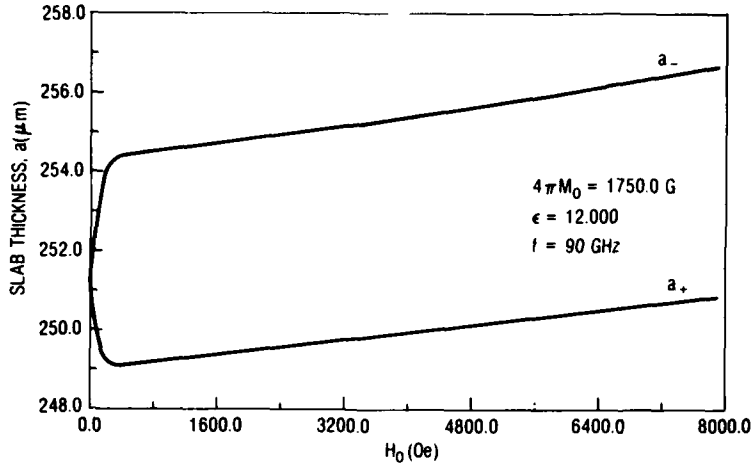

Figure 4. Slab thickness as a function of magnetic field for a hypothetical YIG sample (dielectric constant assumed to be 12).

Figure 5. Slab thickness as a function of magnetic field for a hypothetical YIG sample (dielectric constant assumed to be 14).

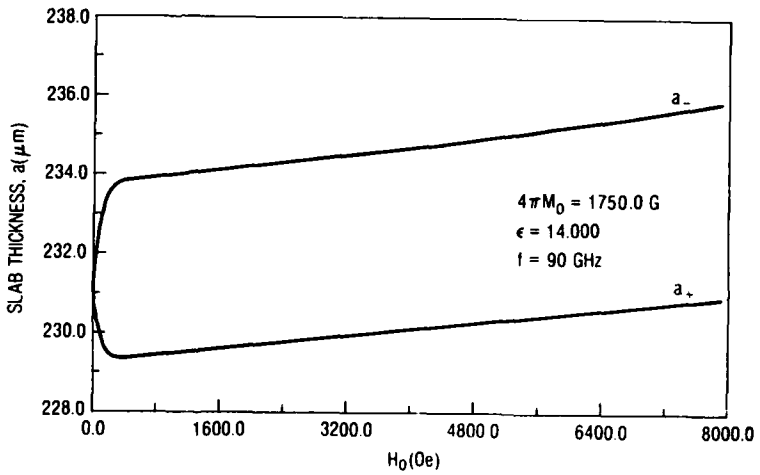

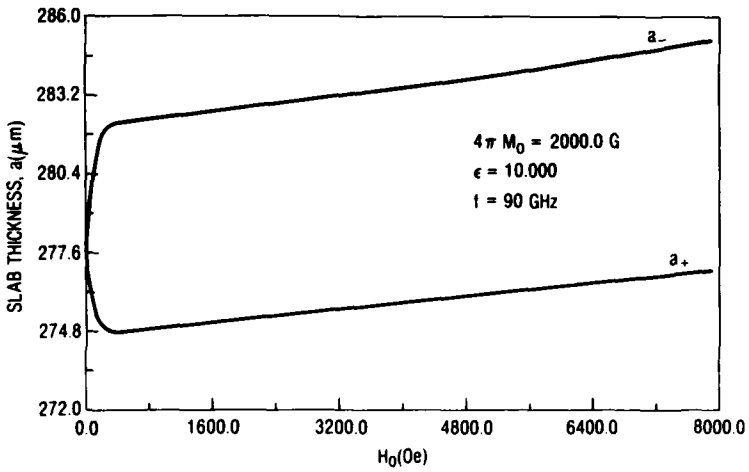

Figure 6. Slab thickness as a function of magnetic field for a hypothetical YIG sample (saturation magnetization assumed to be 2000 G).

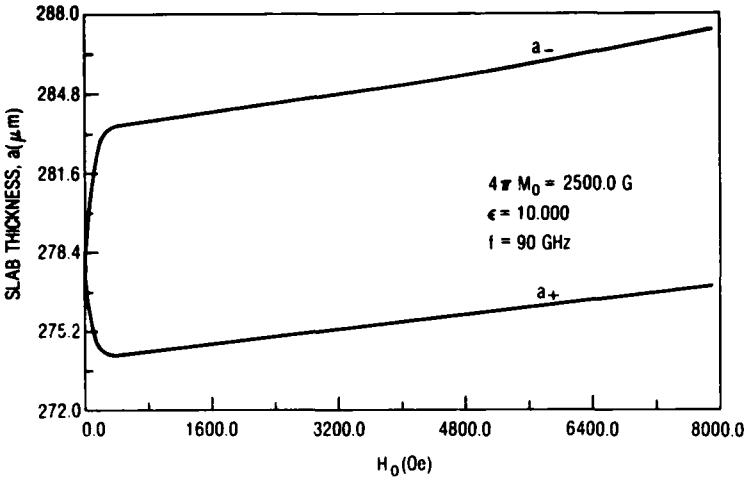

Figure 7. Slab thickness as a function of magnetic field for a hypothetical YIG sample (saturation magnetization assumed to be 2500 G).

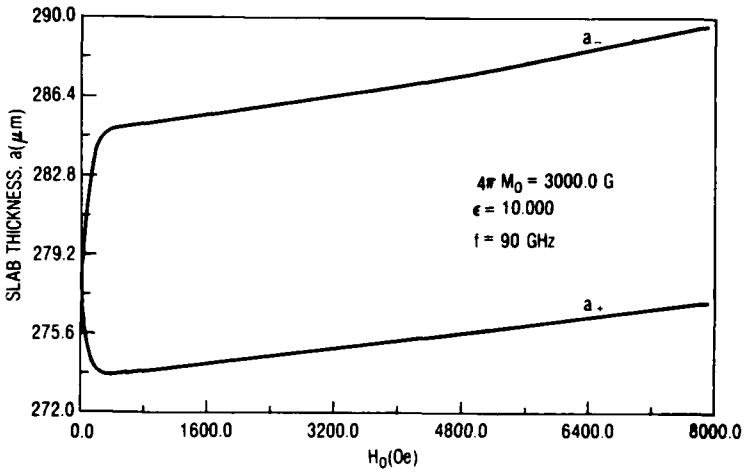

Figure 8. Slab thickness as a function of magnetic field for a hypothetical YIG sample (saturization magnetization assumed to be 3000 G).

Next, the frequency sensitivity of the solutions to equations (20) and (21) are investigated. For the purpose of this investigation YIG was chosen with $\varepsilon = 10$ and $4\pi M_o = 1750$ G as in figure 2. Figure 9 shows the variation of slab thickness, $a_{\pm}$, and differential thickness, Δa, as a function of magnetic field for three different frequencies (80, 90, and 100 GHz). In figure 10 the thickness, $a_{\pm}$, is plotted versus frequency from 80 to 100 GHz for a magnetic field $H_o = 3000$ Oe. The slab thickness for both a_+ and a_- decreases with increasing frequency. Thus, if the dielectric constant decreases with frequency in the correct manner, the slab thickness would remain constant. Unfortunately, ferrites with dispersion in any region of interest have a prohibitive amount of loss in that region.

4. CONCLUSION

We have found the conditions under which a surface wave propagates on a ferrite slab backed by a metal conductor. The only region investigated was that with the static magnetic field much less than the magnetic field required

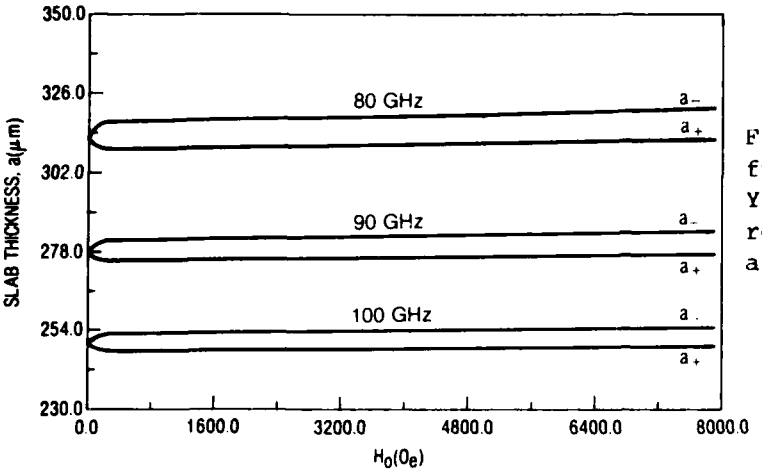

Figure 9. Slab thickness as a function of magnetic field for YIG for three frequencies with reported values of ε and 4πM at X band.

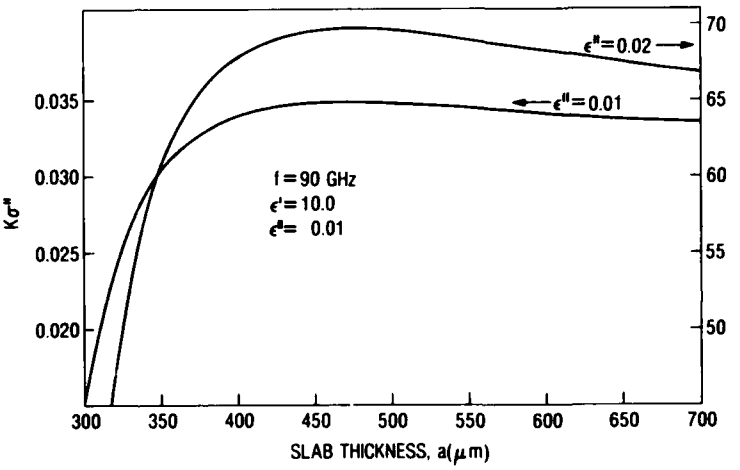

Figure 10. Slab thickness as a function of frequency for YIG with reported values of ε and 4πM at k band.

for ferromagnetic resonance in the material. The results reported here are for the dominant TE mode of the system. Magnetic and dielectric losses were assumed to be negligible in this analysis. It is expected that these results will be useful in the design of a practical device, provided they are used in a region some distance from an abrupt cutoff. The abrupt cutoff points should be softened by the introduction of losses in a manner similar to those used in waveguides when the conductivity of the walls is included.

The results of the analysis are presented in the form of graphs that border the three regions: both forward and reverse propagation but with different phase velocities, only forward propagation, and no propagation. At any given frequency these regions are outlined by slab thickness as a function of applied magnetic field. The forward and reverse propagation in the first region suggests its use as a phase shifter, and the second region can be used for isolation. The third region can be used for switching if the applied magnetic field is suddenly changed from this region to region two.

Losses were considered only for the particular case where the applied magnetic field was zero and magnetic losses were ignored. Small dielectric losses were introduced and the complex propagation constant, $q = q' + iq''$, along the surface was calculated. It was found that for slab thicknesses restricted so that only the dominant mode propagates, the value of q'' was smallest for the minimum slab thickness. A maximum occurred in q'' near the middle range of slab thickness, with q'' gradually decreasing as the thickness of the slab increases.

The predicted slab thickness for YIG falls in the range of thick films which can be fabricated, and perhaps it could be deposited on the conductor by a method similar to liquid phase epitaxy. If single-crystal films are desired, the film probably would have to be deposited on a nonmagnetic single-crystal substrate, such as yttrium gallium garnet, where the crystal cell size matches the magnetic film cell size. In such cases, the analysis of the system would have to be altered considerably from the one presented here.

In further analysis, magnetic as well as dielectric losses in the ferrite slab should be considered. The inclusion of these losses would give the insertion loss for both the phase shifter and isolation mode of operation. Further, for an isolator, the degree of isolation could then be estimated much more realistically.

ACKNOWLEDGEMENTS

We wish to thank Dr. Nick Karayianis for his suggestions at the primitive stage of this work. We also wish to thank Dr. George Simonis for his suggestions and his enthusiastic support throughout this study. We owe thanks also to Dr. Richard Leavitt for much help on the computation. One of us (K.S.) particularly wishes to thank Dr. George Simonis for allowing her time to pursue her part of the work presented here.

Selected Bibliography of Some Earlier Work at HDL on the Theory and Application of Ferrites

L. A. Ault, E. G. Spencer, and R. C. LeCraw, Circularly Polarized Traveling-Wave Cavity for Ferrite Tensor Permeability Measurements, HDL-TR-482 (20 September 1957).

J. C. Cacheris and H. A. Dropkin, Compact Microwave Single-Sideband Modulator using Ferrites, HDL-TR-308 (November 1955).

J. C. Cacheris, G. Jones, and C. A. Morrison, Magnetic Tuning of Resonant Cavities and Wideband Frequency Modulation of Klystrons, HDL-TR-349 (April 1956).

J. C. Cacheris, G. Jones, and R. Van Wolf, Topics in the Microwave Applications of Ferrites, HDL-TR-188 (July 1955).

J. C. Cacheris and N. Karayianis, Birefringence of Ferrites in Circular Waveguide, HDL-TR-347 (April 1956).

J. C. Cacheris and J. Nemarich, Temperature Dependence of Microwave Permeabilities for Polycrystalline Ferrite and Garnet Materials, HDL-TR-647 (October 1958).

J. C. Cacheris and R. Van Wolf, Broadbanding of Microwave Nonreciprocal Ferrite Phase Shifters, HDL-TR-348 (April 1956).

J. C. Cacheris and R. Van Wolf, Compact Ferrite Duplexer-Detector, HDL-TR-712 (June 1959).

R. C. LeCraw and E. G. Spencer, Intrinsic Tensor Permeabilities of Ferrites Below Saturation, HDL-TR-345 (10 May 1954).

R. C. LeCraw and E. G. Spencer, Domain Structure Effects in an Anomalous Ferrimagnetic Resonance of Ferrites, HDL-TR-419 (27 December 1956).

R. C. LeCraw, E. G. Spencer, and C. S. Porter, Ferromagnetic Resonance and Nonlinear Effects in Yttrium Iron Garnet, HDL-TR-541 (12 December 1957).

C. A. Morrison, Perturbation Theory Applied to Samples in a Rectangular Cavity, HDL-TR-298 (9 November 1955).

C. A. Morrison, The Magnetostatic Modes of a Small Hollow Cylinder of Ferrites, HDL-TR-881 (15 November 1960).

J. Nemarich, The Contribution of the Two-Magnon Process to Magnetostatic Mode Relaxation, HDL-TR-1245 (10 August 1964).

J. Nemarich, Measurement of Narrow Magnetic Resonance Linewidths, HDL-TR-1246 (10 August 1964).

J. Nemarich and J. C. Cacheris, Temperature Dependence of Microwave Permeabilities for Polycrystalline Ferrite and Garnet Materials, HDL-TR-647 (3 October 1958).

E. G. Spencer, L. A. Ault, and R. C. LeCraw, Intrinsic-Tensor Permeabilities of Ferrite Rods, Spheres, and Discs, HDL-TR-343 (20 April 1956).

D. E. Wortman, L. A. Ault, and C. A. Morrison, Ferromagnetic Resonance from 300 MC to 10 kMC in Oriented YIG Discs, HDL-TR-992 (8 November 1961).

E. G. Spencer, R. C. LeCraw, and C. S. Porter, Ferromagnetic Resonance in Yttrium Iron Garnet at Low Frequencies, HDL-TR-539 (29 November 1957).

E. G. Spencer, R. C. LeCraw, and C. S. Porter, Microwave Properties of Yttrium Iron Garnet, HDL-TR-633 (30 June 1958).

E. G. Spencer, R. C. LeCraw, and F. Reggia, Measurement of Microwave Dielectric Constants and Tensor Permeabilities of Ferrite Spheres, HDL-TR-344 (25 April 1956).

R. F. Sullivan and R. C. LeCraw, A Broadband Ferrite Microwave Switch, HDL-TR-59 (10 March 1954).

APPENDIX A.--EQUATION OF MOTION OF MAGNETIZATION

The equation of motion of magnetization, as given by Landau and Lifshitz,[1] is

$$\dot{\mathbf{M}}' = \gamma(\mathbf{M}'\times\mathbf{H}') - \frac{\alpha\gamma}{|\mathbf{M}'|}\left[\mathbf{M}'\times(\mathbf{M}'\times\mathbf{H}')\right] \quad , \tag{A-1}$$

where γ is the gyromagnetic ratio and α is the damping constant. The other constants in the second term on the right in equation (A-1) are added for convenience so that α is dimensionless. In most of the materials that we consider, the damping is small and it is convenient to use Gilbert's approximation.[2] That is, in the second term on the right we assume that

$$\mathbf{M}'\times\mathbf{H}' \simeq \frac{1}{\gamma}\dot{\mathbf{M}}' \quad . \tag{A-2}$$

The equation (A-1) becomes

$$\dot{\mathbf{M}}' = \gamma(\mathbf{M}'\times\mathbf{H}') - \frac{\alpha}{|\mathbf{M}'|}(\mathbf{M}'\times\dot{\mathbf{M}}') \quad . \tag{A-3}$$

The result given in equation (A-3) agrees with the result of equation (A-1), if terms of order α^2 and higher are ignored. At the low power levels that we considered, it is sufficient to linearize equation (A-3) by letting

$$\mathbf{H}' = \hat{e}_z H_o + \mathbf{H}''$$

and

$$\mathbf{M}' = \hat{e}_z M_o + \mathbf{M}'' \quad , \tag{A-4}$$

with the conditions

$$|\mathbf{H}''| \ll H_o$$

and

$$|\mathbf{M}''| \ll M_o \quad .$$

In this equation $\hat{e}_z$ is a unit vector along the z-axis. In equation (A-4), we assume the static magnetic field, H_o, and the static magnetization, M_o, to be in the z direction. The assumption of small amplitude signals also leads to $\mathbf{M}''$ and $\mathbf{H}''$ having only components transverse to z.

If we use equation (A-4) in equation (A-3) we have

$$\dot{\mathbf{M}}'' = \gamma\left(\dot{\mathbf{M}}''\times\hat{e}_z H_o + \hat{e}_z M_o\times\mathbf{H}''\right) - \frac{\alpha}{M_o}\left(\hat{e}_z M_o\times\dot{\mathbf{M}}''\right) \quad , \tag{A-5}$$

where we assume that $|\mathbf{M}| \simeq M_o$. We assume that all the time-varying quantities have a harmonic time dependence, $e^{-i\omega t}$, and we let

---

[1] *L. Landau and L. Lifshitz, On the Theory of the Dispersion of Magnetic Permeability in Ferromagnetic Bodies, Physik Zeitschrift Sowjetunion, 8 (1935), 153.*

[2] *T. A. Gilbert, Armour Research Foundation, Rept. No. 11 (January 25, 1955).*

APPENDIX A

$$\mathbf{M}'' = \mathbf{M}e^{-i\omega t}$$

and (A-6)

$$\mathbf{H}'' = \mathbf{H}e^{-i\omega t} \quad ,$$

with **M** and **H** time independent but still spatially dependent. Using equation (A-6) in equation (A-5) and expressing the results in Cartesian components gives

$$-i\omega M_x = \gamma\left(M_y H_o - M_o H_y\right) - i\omega\alpha M_y$$

and (A-7)

$$-i\omega M_y = \gamma\left(M_o H_x - M_x H_o\right) + i\omega\alpha M_x \quad .$$

To obtain the relation of **M** to **H**, it is convenient to use the circular polarized quantities,

$$M_\pm = M_x \pm iM_y$$

and (A-8)

$$H_\pm = H_x \pm iH_y \quad .$$

Substituting equation (A-8) into equation (A-7) we obtain

$$M_\pm = \frac{\mp\gamma M_o H_\pm}{\omega(1 \pm i\alpha) \mp \gamma H_o} \quad . \tag{A-9}$$

In the cgs system the relationship of **B**, **H**, and **M** is

$$\mathbf{B} = \mathbf{H} + 4\pi\mathbf{M} \tag{A-10}$$

so that we can write

$$B_\pm = \mu_\pm H_\pm \quad .$$

From equations (A-10) and (A-9)

$$\mu_\pm = 1 \mp \frac{\gamma 4\pi M_o}{\omega(1 \pm i\alpha) \mp \gamma H_o} \quad . \tag{A-11}$$

The properties of ferromagnetic materials are characterized by $4\pi M_o$ and α. However, the damping parameter α is replaced frequently by the linewidth, measured at constant frequency as a function of H_o. The parameter α is then related to the linewidth, ΔH, by

$$\alpha = \frac{\gamma\Delta H}{\omega} \quad , \tag{A-12}$$

where ΔH is *half* of the full linewidth at half maximum of the absorption. Sometimes the *full* linewidth at half maximum of the absorption is reported; thus, equation (A-12) must be used with caution.

The circular polarization form of the magnetic permeability is convenient for electromagnetic boundary value problems when the ferrite material has circular symmetry about the static magnetic field, H_o. However, for our problem, the permeability tensor relation of **B** and **H** is more convenient. This relation is usually written as

$$B_x = \mu H_x + i\kappa H_y$$

and (A-13)

$$B_y = \mu H_y - i\kappa H_x \quad .$$

From equation (A-11) we find

$$\mu = (\mu_+ + \mu_-)/2$$

and (A-14)

$$\kappa = (\mu_+ - \mu_-)/2 \quad .$$

For the case where α is small and the static magnetic field is far below resonance ($\gamma H_o << \omega$), we have

$$\mu \simeq 1 - \frac{\gamma H_o \gamma(4\pi M_o)}{\omega^2} + i\alpha \frac{\gamma(4\pi M_o)}{\omega}$$

and

$$\kappa \simeq - \frac{\gamma(4\pi M_o)}{\omega} + 2i\alpha \frac{\gamma H_o \gamma(4\pi M_o)}{\omega^2} \quad .$$

APPENDIX B.--THE LOSSES IN A DIELECTRIC SLAB

During the course of this investigation we consider only lossless material. The reason for this assumption is the difficulty of developing a general technique for examining the roots of the resulting transcendental equation which determine the modes of propagation (an example is (13) in the main text).

In this appendix we examine the consequence of assuming that the magnetic field is zero and the only source of losses is the dielectric. Further, if we assume the losses are small, the resulting equations for determining the propagation constant can be solved by a perturbation technique. We assume that the dielectric constant is given by

$$\varepsilon = \varepsilon' + i\varepsilon'' \tag{B-1}$$

and further assume that $\varepsilon'' << \varepsilon'$. If we let $H = 0$ ($\mu = 1$, $\kappa = 0$) in equation (13) in the main text, we obtain

$$\gamma_i \cot\left(ka\gamma_i\right) = -\gamma_o \tag{B-2}$$

with

$$\gamma_i^2 + \gamma_o^2 = \varepsilon - 1$$

and

$$\sigma^2 = 1 + \gamma_o^2 \ .$$

Now if we assume

$$\gamma_i = \gamma_i' + i\gamma_i'' \ ,$$

$$\gamma_o = \gamma_o' + i\gamma_o'' \ , \tag{B-3}$$

and

$$\sigma = \sigma' + i\sigma''$$

with all the imaginary parts small compared to the real parts, then

$$\cot\left(ka\gamma_i\right) \simeq \cot\left(ka\gamma_i'\right) - ika\gamma_i''\left[1 + \cot^2\left(ka\gamma_i'\right)\right] \tag{B-4}$$

and

$$\gamma_o' + i\gamma_o'' = \gamma_o' + \frac{i\left(\varepsilon'' - 2\gamma_i'\gamma_i''\right)}{\gamma_o'} \ . \tag{B-5}$$

Thus the real part of equation (B-2) satisfies

$$\gamma_i' \cot\left(ka\gamma_i'\right) = -\gamma_o' \ , \tag{B-6}$$

so that the real part of γ_i' satisfies the same equation as equation (B-2) when γ_i is replaced by γ_i'. The imaginary parts of equations (B-4) and (B-5)

satisfy

$$ka\gamma_i''\left[1 + \cot^2\left(\kappa a\gamma_i'\right)\right] = \left(\varepsilon'' - 2\gamma_i'\gamma_i''\right)/\gamma_o' \quad , \tag{B-7}$$

which can be further reduced by using equation (B-6) and

$$\gamma_i'^2 + \gamma_o'^2 = \varepsilon' - 1$$

to give

$$\gamma_i'' = \frac{\varepsilon''\gamma_i'}{2\left(\varepsilon' - 1\right)\left(1 + \kappa a\gamma_o'\right)} \quad . \tag{B-8}$$

The remainder of the imaginary parts of the quantities of equation (B-3) can be obtained by using the result given in equations (B-8) and (B-2) to give

$$\begin{aligned} \gamma_o'' &= \left(\varepsilon''/2 - \gamma_i'\gamma_i''\right)/\gamma_o' \quad , \\ \sigma' &= \left(1 + \gamma_o'^2\right)^{1/2} \quad , \end{aligned} \tag{B-9}$$

and

$$\sigma'' = \gamma_o'\gamma_o''/\sigma' \quad .$$

Thus, once the solutions of equation (B-6) are determined, the quantities given in equations (B-8) and (B-9) can be determined.

The solution for equation (B-6) has been obtained for $\varepsilon' = 10$ and $\varepsilon'' = 0.01$ for the dominant mode. The region of interest of thickness a in equation (B-6) is easily shown to be

$$\frac{\pi}{2k\sqrt{\varepsilon' - 1}} \leq a \leq \frac{3\pi}{2k\sqrt{\varepsilon' - 1}} \quad , \tag{B-10}$$

where for smaller thickness than the lower limit no surface wave propagates, while for larger thickness than the upper limit both the dominant mode and higher modes propagate. The solution for equation (B-6) for f = 90 GHz, $\varepsilon' = 10$, and $\varepsilon'' = 0.01$ for values of a in the interval is given by equation (B-10). The results for q" ($q'' = k\sigma''$) are shown in figure B-1. Since all the yield quantities vary as $e^{ik\sigma y}$, σ'' gives the decay of the fields in the direction of propagation as $e^{-k\sigma''|y|}$. The results show that for thin slabs (a near the lower limit in eq (B-10)) the attenuation is small. As the slab thickness increases, the attenuation increases, reaching a maximum, and then decreases as a approaches the upper limit in equation (B-10). Also shown is the same calculation with $\varepsilon'' = 0.02$ and all other quantities unchanged. During the course of the computation all the imaginary parts in equation (B-3) were monitored and found to be small compared to the real part of the corresponding quantities. Thus the results are valid for the entire range of a given in equation (B-10).

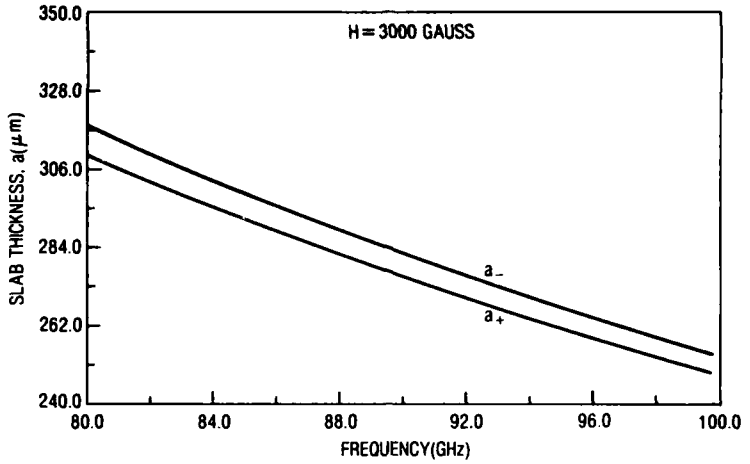

Figure B-1. Imaginary part of propagation constant, $q = q' + iq''$, with $\varepsilon' = 10$ and $\varepsilon'' = 0.1$, or at 90 GHz. Slab thickness restricted so that only dominant mode propagates.

DISTRIBUTION

ADMINISTRATOR
DEFENSE TECHNICAL INFORMATION CENTER
ATTN DTIC-DDA (12 COPIES)
CAMERON STATION, BUILDING 5
ALEXANDRIA, VA 22314

DIRECTOR
DEFENSE ADVANCED RESEARCH PROJECTS AGENCY
ARCHITECT BLDG
ATTN MATERIALS SCIENCES
ATTN ADVANCED CONCEPTS DIV
ATTN TARGET ACQUISITION & ENGAGEMENT DIV
ATTN TTO, DR. J. TEGNELIA
ATTN STO, DR. S. ZAKANYCZ
1400 WILSON BLVD
ARLINGTON, VA 22209

INSTITUTE FOR DEFENSE ANALYSIS
ATTN DR. V. J. CORCORAN
1801 N. BEAUREGARD ST
ALEXANDRIA, VA 22311

DIRECTOR
DEFENSE COMMUNCATIONS AGENCY
ATTN TECHNICAL LIBRARY
ATTN COMMAND & CONTROL CENTER
WASHINGTON, DC 20305

DIRECTOR
DEFENSE COMMUNICATIONS ENGINEERING CENTER
ATTN TECHNICAL LIBRARY
1860 WIEHLE AVENUE
RESTON, VA 22090

DIRECTOR
NATIONAL SECURITY AGENCY
ATTN TECHNICAL LIBRARY
FT MEADE, MD 20755

OUSDR&E
DIRECTOR ENERGY TECHNOLOGY OFFICE
THE PENTAGON
WASHINGTON, DC 20301

OUSDR&E
ASSISTANT FOR RESEARCH
THE PENTAGON
WASHINGTON, DC 20301

OFFICE OF THE DEPUTY CHIEF OF STAFF FOR RESEARCH, DEVELOPMENT, & ACQUISITION
ATTN DIR OF ARMY RES, DAMA-ARZ-A DR. M. E. LASSER
ATTN DAMA-E, ADVANCED CONCEPTS TEAM
WASHINGTON, DC 20310

COMMANDER
US ARMY ARMAMENT MATERIEL READINESS COMMAND
ATTN DRSAR-LEP-L, TECHNICAL LIBRARY
ATTN DRSAR-ASF, FUZE & MUNITIONS SUPPORT DIV
ROCK ISLAND, IL 61299

COMMANDER
US ARMY ATMOSPHERIC SCIENCES LABORATORY
ATTN DRSEL-BL-AS-P, DR. K. WHITE
WHITE SANDS MISSILE RANGE, NM 88002

COMMANDER
BALLISTIC MISSILE DEFENSE AGENCY
ADVANCED TECHNOLOGY CENTER
ATTN BMD-ATC-D, C. JOHNSON
PO BOX 1500
HUNTSVILLE, AL 35807

DIRECTOR
US ARMY BALLISTIC RESEARCH LABORATORY
ATTN DRDAR-TSB-S (STINFO)
ATTN DRDAR-BLB, R. MCGEE
ATTN DRDAR-BL, H. REED
ABERDEEN PROVING GROUND, MD 21005

COMMANDER
US ARMY COMMUNICATIONS & ELECTRONICS MATERIEL READINESS COMMAND
ATTN H. JACOBS
ATTN V. G. GELNOVATCH
ATTN R. STERN
FT MONMOUTH, NJ 07703

COMMANDER
EDGEWOOD ARSENAL
ABERDEEN PROVING GROUND, MD 21005

DIRECTOR
ELECTRONIC WARFARE LABORATORY
ATTN DELEW-SM, EW SYSTEMS MGT OFFICE
ATTN DELEW-C, COMM INTEL/CM DIV
ATTN DELEW-E, ELCT INTEL/CM DIV
FT MONMOUTH, NJ 07703

US ARMY ELECTRONICS TECHNOLOGY & DEVICES LABORATORY
ATTN DELET-DD
FT MONMOUTH, NJ 07703

COMMANDER
US ARMY ELECTRONICS PROVING GROUND
FT HUACHUCA, AZ 85613

COMMANDER/DIRECTOR
ATMOSPHERIC SCIENCES LABORATORY
US ARMY ERADCOM
ATTN DELAS-EO, ELECTRO-OPTICS DIVISION
WHITE SANDS MISSILE RANGE, NM 88002

COMMANDER/DIRECTOR
COMBAT SURVEILLANCE
& TARGET ACQUISITION LABORATORY
US ARMY ERADCOM
ATTN DELCS-DT, CHIEF TECHNICAL PLANS & MGT OFFICE
ATTN DELCS-R, DIR RADAR DIV
FT MONMOUTH, NJ 07703

COMMANDER
ERADCOM TECHNICAL SUPPORT ACTIVITY
ATTN DELSD-L, TECH LIB DIR
FT MONMOUTH, NJ 07703

DIRECTOR
ELECTRONICS TECHNOLOGY &
DEVICES LABORATORY
US ARMY ERADCOM
ATTN DELET-DT, DIR TECHNICAL PLANS & PROGRAMS OFFICE
ATTN DELET-E, DIR ELECTRONIC MATERIALS RESEARCH DIV
ATTN DELET-I DIR MICROELECTRONICS DIV
ATTN DELET-M, MICROWAVE & SIGNAL PROCESSING DEVICES DIV
FT MONMOUTH, NJ 07703

COMMANDER
US ARMY ERADCOM
ATTN DRSEL-TL-IJ, DR. A. KERECMAN
ATTN DRSEL-CT-R, R. PEARCE
ATTN DRSEL-CT-L, DR. ROHDE
FT MONMOUTH, NJ 07703

US ARMY FOREIGN SCIENCE & TECHNOLOGY CENTER
ATTN DRXST-SD, DR. O. R. HARRIS
220 SEVENTH STREET, NE
CHARLOTTESVILLE, VA 22901

COMMANDER
US ARMY FRANKFORD ARSENAL
ATTN SARFA N5100, J. LESTER
BLDG 201-3
BRIDGE-TACONY STS
PHILADELPHIA, PA 91937

COMMANDER
US ARMY INTELLIGENCE & SEC COMMAND
ATTN TECH LIBRARY
ARLINGTON HALL STATION
4000 ARLINGTON BLVD
ARLINGTON, VA 22212

COMMANDER
US ARMY MATERIEL DEVELOPMENT & READINESS COMMAND
ATTN DRCBSI, DR. P. DICKINSON
ATTN DRCPA, DIR FOR PLANS & ANALYSIS
ATTN DRCDE, DIR FOR DEVELOPMENT & ENG
5001 EISENHOWER AVE
ALEXANDRIA, VA 22333

COMMANDER
US ARMY MATERIALS & MECHANICS RESEARCH CENTER
ATTN DRXMR-PL, TECHNICAL LIBRARY
WATERTOWN, MA 02172

DIRECTOR
US ARMY MATERIEL SYSTEMS ANALYSIS ACTIVITY
ATTN DRXSY-MP
ABERDEEN PROVING GROUND, MD 21005

COMMANDER
US ARMY MIRADCOM
ATTN DRDMI-TRO, DR. W. L. GAMBLE
ATTN DRDMI-TRO, DR. B. D. GUENTHER
ATTN DRSMI-REO, DR. G. EMMONS
REDSTONE ARSENAL, AL 35809

COMMANDER
US ARMY MISSILE COMMAND
ATTN DRSMI-RLA, K. LETSON
ATTN DRSMI-RLA, D. HARTMAN
REDSTONE ARSENAL, AL 35898

COMMANDER
US ARMY MISSILE & MUNITIONS CENTER & SCHOOL
ATTN ATSK-CTD-F
REDSTONE ARSENAL, AL 35809

COMMANDER
US ARMY NATICK RES & DEV COMMAND
NATICK DEVELOPMENT CENTER
ATTN DRDNA-T, TECHNICAL LIBRARY
NATICK, MA 01760

DIRECTOR
NIGHT VISION & ELECTRO-OPTICS
LABORATORY
ATTN DELNV-IRT, INFRARED TECHNOLOGY DIV
ATTN DELNV-[illegible], ASSESSMENT DIVISION
ATTN DELNV-[illegible]
ATTN DELNV-[illegible]
ATTN DELNV-[illegible]
ATTN [illegible]
ATTN [illegible]
ATTN [illegible]
ATTN [illegible]

COMMANDER
US ARMY NUCLEAR & CHEMICAL AGENCY
ATTN ATCN-W, WEAPONS EFFECTS DIV
7500 BACKLICK ROAD
BUILDING 2073
SPRINGFIELD, VA 22150

COMMANDER/DIRECTOR
CHEMICAL SYSTEMS LABORATORY
ARRADCOM
ATTN DRDAR-CLJ-L, TECHNICAL LIBRARY BRANCH
ABERDEEN PROVING GROUND, MD 21010

COMMANDER
US ARMY RSCH & STD GP (EUR)
ATTN CHIEF, PHYSICS & MATH BRANCH
FPO NEW YORK 09510

DIRECTOR
US ARMY RESEARCH & TECHNOLOGY
LABORATORIES
AMES RESEARCH CENTER
MOFFETT FIELD, CA 94035

US CHIEF ARMY RESEARCH OFFICE (DURHAM)
PO BOX 12211
ATTN DRXRO-EL, DIR ELECTRONICS DIV
ATTN DRXRO-PH, DIR PHYSICS DIV
ATTN DRXRO-MS, METALLURGY-MATERIALS
DIV
RESEARCH TRIANGLE PARK, NC 27709

DIRECTOR
PROPULSION LABORATORY
RESEARCH & TECHNOLOGY LABORATORIES
AVRADCOM
LEWIS RESEARCH CENTER, MS. 106-2
21000 BROOKPARK ROAD
CLEVELAND, OH 44135

DIRECTOR
APPLIED TECHNOLOGY LABORATORY
AVRADCOM
ATTN DAVDL-ATL-TSD, TECH LIBRARY
FT EUSTIS, VA 23604

ASSISTANT SECRETARY OF THE NAVY
RESEARCH, ENGINEERING, & SYSTEMS
DEPT OF THE NAVY
WASHINGTON, DC 20350

CHIEF OF NAVAL RESEARCH
DEPT OF THE NAVY
ATTN ONR-400, ASST CH FOR RES
ATTN ONR-420, PHYSICAL SCI DIV
ARLINGTON, VA 22217

COMMANDER
NAVAL RESEARCH LAB
ATTN B. YAPLEE, CODE 7110
ATTN DR. J. P. HOLLINGER, CODE 7111
ATTN DR. K. SHIVANANDAN, CODE 7122.1
WASHINGTON, DC 20375

SUPERINTENDENT
NAVAL POSTGRADUATE SCHOOL
ATTN LIBRARY, CODE 2124
MONTEREY, CA 93940

DIRECTOR
NAVAL RESEARCH LABORATORY
ATTN 2600, TECHNICAL INFO DIV
ATTN 2750, OPTICAL SCIENCES DIV
ATTN 5500, OPTICAL SCI DIV
ATTN 6000, MATL & RADIATION
SCI & TE
WASHINGTON, DC 20375

COMMANDER
NAVAL SURFACE WEAPONS CENTER
ATTN DX-21, LIBRARY DIV
DAHLGREN, VA 22448

COMMANDING OFFICER
NAVAL TRAINING EQUIPMENT CENTER
ATTN TECHNICAL LIBRARY
ORLANDO, FL 32813

COMMANDER
NAVAL WEAPONS CENTER
ATTN 38, RESEARCH DEPT
ATTN 381, PHYSICS DIV
CHINA LAKE, CA 93555

HQ, USAF/SAMI
WASHINGTON, DC 20330

DEPUTY CHIEF OF STAFF
RESEARCH & DEVELOPMENT
HEADQUARTERS, US AIR FORCE
ATTN AFRDQSM
WASHINGTON, DC 20330

SUPERINTENDENT
HQ US AIR FORCE ACADEMY
ATTN TECH LIB
USAF ACADEMY, CO 80840

COMMANDER
AIR FORCE AVIONICS LABORATORY
ATTN KJA (TEO), ELECTRO-OPTICS
TECHNOLOGY BR
WRIGHT-PATTERSON AFB, OH 45433

HQ AF DATA AUTOMATION AGENCY
ATTN DATA SYS EVAL OFFICE
GUNTER AFS, AL 36114

DISTRIBUTION (Cont'd)

COMMANDER
HQ ROME AIR DEVELOPMENT CENTER (AFSC)
ATTN LE, DEPUTY FOR ELECTRONIC TECH
ATTN LMT, TELECOMMUNICATIONS BR
GRIFFISS AFB, NY 13441

COMMANDER
AF ELECTRONIC SYSTEMS DIVISION
ATTN WO, DEP FOR CONTROL
& COMMUNICATIONS SYS
L. G. HANSCOM AFB, MA 01730

COMMANDER
US AIR FORCE GEOPHYSICAL LAB
L. G. HANSCOMB FIELD
ATTN DR. S. A. CLOUGH
BEDFORD, MA 01731

DIRECTOR
AF OFFICE OF SCIENTIFIC RESEARCH
BOLLING AFB
ATTN NE, DIR OF ELECTRONIC &
SOLID STATE SCI
WASHINGTON, DC 20332

COMMANDER
US AIR FORCE ROME AIR DEVELOPMENT
CENTER
ATTN RADC/ETEN, DR. E. ALTSHULER
L. G. HANSCOM FIELD
BEDFORD, MA 01730

COMMANDER
HQ AIR FORCE SYSTEMS COMMAND
ANDREWS AFB
ATTN TECHNICAL LIBRARY
WASHINGTON, DC 20334

AF WEAPONS LABORATORY, AFSC
ATTN EL, ELECTRONICS DIV
ATTN LR, LASER DEV DIV
KIRTLAND AFB, NM 87117

AMES RESEARCH CENTER
NASA
ATTN TECHNICAL INFO DIV
MOFFETT FIELD, CA 94035

DIRECTOR
NASA
GODDARD SPACE FLIGHT CENTER
ATTN 250, TECH INFO DIV
GREENBELT, MD 20771

DIRECTOR
NASA
ATTN TECHNICAL LIBRARY
JOHN F. KENNEDY SPACE
CENTER, FL 32899

DIRECTOR
NASA
LANGLEY RESEARCH CENTER
ATTN TECHNICAL LIBRARY
HAMPTON, VA 23665

DIRECTOR
NASA
LEWIS RESEARCH CENTER
ATTN TECHNICAL LIBRARY
CLEVELAND, OH 44135

DEPARTMENT OF COMMERCE
NATIONAL BUREAU OF STANDARDS
ATTN LIBRARY
WASHINGTON, DC 20230

NATIONAL OCEANIC & ATMOSPHERIC ADM
ENVIRONMENTAL RESEARCH LABORATORIES
ATTN LIBRARY, R-51, TECH REPORTS
BOULDER, CO 80302

INSTITUTE FOR TELECOMMUNICATIONS
SCIENCES
NATIONAL TELECOMMUNICATIONS &
INFO ADMIN
ATTN LIBRARY
BOULDER, CO 80303

THE AEROSPACE CORPORATION
THE IVAN A. GETTING LAB
ATTN DR. T. S. HARTWICK
ATTN DR. D. T. HODGES
PO BOX 92957
LOS ANGELES, CA 90009

ENGINEERING SOCIETIES LIBRARY
ATTN ACQUISITIONS DEPARTMENT
345 EAST 47TH STREET
NEW YORK, NY 10017

ENVIRONMENTAL RESEARCH INSTITUTE OF
MICHIGAN
ATTN DR. GWYNN H. SUITS
PO BOX 618
ANN ARBOR, MI 48107

FORD-AERONUTRONIC
ATTN DR. D. E. BURCH
FORD ROAD
NEWPORT BEACH, CA 92663

HONEYWELL CORPORATE RESEARCH CENTER
ATTN DR. P. W. KRUSE
10701 LYNDALE AVE S
BLOOMINGTON, MN 55420

LAWRENCE LIVERMORE NATIONAL LABORATORY
PO BOX 808
LIVERMORE, CA 94550

DISTRIBUTION (Cont'd)

NATIONAL OCEANGRAPHIC & ATMOSPHERIC
ADMINISTRATION
ATTN DR. V. E. DERR
BOULDER, CO 80303

R&D ASSOCIATES
ATTN DR. G. GORDON
PO BOX 9695
MARINA DEL REY, CA 90291

SANDIA LABORATORIES
LIVERMORE LABORATORY
PO BOX 969
LIVERMORE, CA 94550

SANDIA NATIONAL LABORATORIES
PO BOX 5800
ALBUQUERQUE, NM 87185

JET PROPULSION LABORATORY
CALIFORNIA INSTITUTE OF TECHNOLOGY
4800 OAK GROVE DRIVE
ATTN TECHNICAL LIBRARY
PASADENA, CA 91103

GEORGIA INSTITUTE OF TECHNOLOGY
ENGINEERING EXPERIMENT STATION
ATTN J. J. GALLAGHER
ATLANTA, GA 30332

UNIVERSITY OF CALIFORNIA
SCHOOL OF ENGINEERING
LOS ANGELES, CA 90024

CATHOLIC UNIVERSITY OF AMERICA
CARDINAL STATION
PO BOX 232
WASHINGTON, DC 20017

UNIVERSITY OF ILLINOIS
DEPT OF ELECTRICAL ENGINEERING, 200 EERL
ATTN DR. P. D. COLEMAN
ATTN DR. T. A. DETEMPLE
URBANA, IL 61801

MIT
FRANCIS BITTER NATIONAL MAGNET LAB
ATTN K. J. BUTTON
170 ALBANY STREET
CAMBRIDGE, MA 02139

MIT
LINCOLN LAB
ATTN C. BLAKE
PO BOX 73
LEXINGTON, MA 02173

CIVIL ENGINEERING RESEARCH FACILITY
UNIVERSITY OF NEW MEXICO
PO BOX 188
ALBUQUERQUE, NM 87131

RUTGERS UNIVERSITY
COLLEGE OF ENGINEERING
DEPARTMENT OF CERAMICS
NEW BRUNSWICK, NJ 08903

MS. KARLA SORENSON (10 COPIES)
90 JENNESS STREET
LOWELL, MA 01851

US ARMY ELECTRONICS RESEARCH
& DEVELOPMENT COMMAND
ATTN COMMANDER, DRDEL-CG
ATTN TECHNICAL DIRECTOR, DRDEL-CT
ATTN PUBLIC AFFAIRS OFFICE, DRDEL-IN

HARRY DIAMOND LABORATORIES
ATTN CO/TD/TSO/DIVISON DIRECTORS
ATTN RECORD COPY, 81200
ATTN HDL LIBRARY, 81100 (3 COPIES)
ATTN HDL LIBRARY, 81100 (WOODBRIDGE)
ATTN TECHNICAL REPORTS BRANCH, 81300
ATTN LEGAL OFFICE, 97000
ATTN CHAIRMAN, EDITORIAL COMMITTEE
ATTN B. ZABLUDOWSKI, 47400 (GIDEP)
ATTN C. LANHAM, 00213
ATTN S. ELBAUM, 97100
ATTN J. NEMARICH, 13300
ATTN S. M. KULPA, 13300
ATTN B. A. WEBER, 13300
ATTN H. E. BRANDT, 22300
ATTN Z. G. SZTANKAY, 13300
ATTN F. G. FARRAR, 11200
ATTN W. G. WIEBACH, 11200
ATTN R. CHASE, 15300
ATTN T. WATT, 11200
ATTN D. GIGLIO, 15300
ATTN G. CIRINCIONE, 15300
ATTN W. TRUEHART, 11100
ATTN D. E. WORTMAN, 13200
ATTN M. S. TOBIN, 13200
ATTN R. P. LEAVITT, 13200
ATTN F. J. CROWNE, 13200
ATTN H. DROPKIN, 13200
ATTN P. S. BRODY, 13200
ATTN G. T. SIMONIS, 13200
ATTN J. P. SATTLER, 13200
ATTN A. F. HANSEN, 13200 (10 COPIES)
ATTN C. A. MORRISON, 13200 (10 COPIES)

END

FILMED

9-83

DTIC